Developmental Cell
Article

Interaction between Meristem Tissue Layers Controls Phyllotaxis

Daniel Kierzkowski,[1,3] Michael Lenhard,[2] Richard Smith,[1,3] and Cris Kuhlemeier[1,*]
[1]Institute of Plant Sciences, University of Bern, Bern CH-3013, Switzerland
[2]Institute of Biochemistry and Biology, University of Potsdam, Potsdam 14476, Germany
[3]Present address: Max Planck Institute for Plant Breeding Research, Köln 50829, Germany
*Correspondence: cris.kuhlemeier@ips.unibe.ch
http://dx.doi.org/10.1016/j.devcel.2013.08.017

SUMMARY

Phyllotaxis and vein formation are among the most conspicuous patterning processes in plants. The expression and polarization of the auxin efflux carrier PIN1 is the earliest marker for both processes, with mathematical models indicating that PIN1 can respond to auxin gradients and/or auxin flux. Here, we use cell-layer-specific PIN1 knockouts and partial complementation of auxin transport mutants to examine the interaction between phyllotactic patterning, which occurs primarily in the L1 surface layer of the meristem, and midvein specification in the inner tissues. We show that PIN1 expression in the L1 is sufficient for correct organ positioning, as long as the L1-specific influx carriers are present. Thus, differentiation of inner tissues can proceed without PIN1 or any of the known polar transporters. On theoretical grounds, we suggest that canalization of auxin flux between an auxin source and an auxin sink may involve facilitated diffusion rather than polar transport.

INTRODUCTION

Leaves and flowers are initiated at the shoot apical meristem. This dome-shaped structure can be functionally divided into three regions: (1) a slowly growing central zone containing the stem cell niche; (2) the surrounding peripheral zone, where organ initiation takes place; and (3) the rib meristem located underneath the central zone, which is responsible for production of internal tissue of the stem (Rieu and Laux, 2009; Sablowski, 2011; Steeves and Sussex, 1989). When examined in longitudinal sections, meristems display tissue stratification. For instance, the *Arabidopsis thaliana* meristem consists of three well-defined cell layers: the outermost, highly organized L1 and L2 layers, subtended by a less structured internal tissue, the L3. These structural differences are due to preferential anticlinal orientations of cell divisions in the two outer layers of the meristem (Rieu and Laux, 2009; Steeves and Sussex, 1989). Additionally, the L1 layer is characterized by a set of genes that specify outer cell layer identity (Ingram, 2004).

Meristems initiate lateral organs, leaves or flowers, at highly characteristic divergence angles, a phenomenon known as phyllotaxis (Kuhlemeier, 2007; Traas, 2013). One major theory of phyllotaxis posits that all information for correct patterning is contained within the meristem, that is, the meristem is a self-organizing ''patterning machine'' that does not rely on signals from the differentiated tissues below. This theory is supported by classical experiments, in which meristems that were dissected from the subtending tissue continued to produce lateral organs in correct positions (Steeves and Sussex, 1989). More recent experiments further support this view. Auxin induces lateral organs and the first sign of organ positioning is the formation of auxin maxima in the L1 layer of the peripheral zone (Benková et al., 2003; Heisler et al., 2005; Reinhardt et al., 2003). The formation of auxin maxima is thought to involve a positive feedback loop between auxin and one of its transporters, the PIN1 efflux carrier. Indeed, mathematical modeling shows that auxin redistribution by PIN1 exclusively within the L1 surface layer of the meristem can fully recapitulate all major phyllotactic patterns (Jönsson et al., 2006; Smith et al., 2006).

However, other data suggest that organ positioning at the meristem is influenced by signals from below. Anatomical studies have shown that the sites of lateral organ formation at the meristem closely match the positions of the subtending leaf traces (Esau, 1965; Kang et al., 2003; Larson, 1975) and that signals originating from below affect meristem organization (Stuurman et al., 2002; Tucker et al., 2008). Vein patterning is also thought to result from a feedback of auxin on its own transport (Mitchison, 1980; Sachs, 1981). The expression of PIN1 and the auxin reporter DR5 is initially in a cone-shaped area of the meristem below the site of the incipient organ, which subsequently narrows and acquires procambial identity (Baima et al., 1995; Bayer et al., 2009; Scarpella et al., 2004, 2006). PIN1 activity and DR5 reporter expression are the earliest known markers for both patterning processes, and their temporal separation has remained elusive. Thus, an unanswered question is whether the auxin maximum in the L1 layer determines the position of the midvein or vice versa. Simulation models typically use a two-dimensional longitudinal section of the meristem for modeling vein initiation (Bayer et al., 2009; Mitchison, 1980; Rolland-Lagan and Prusinkiewicz, 2005) or the L1 surface layer for modeling phyllotaxis (Heisler and Jönsson, 2006; Smith et al., 2006; Stoma et al., 2008). Since the patterning of lateral organs and the midvein are tightly linked, in both space and time (Bayer et al., 2009; Heisler et al., 2005; Reinhardt et al., 2003), it is possible that the patterning of lateral organ formation requires simultaneous specification of all three axes, making it a genuine three-dimensional patterning phenomenon.

PIN1 is the best characterized component of both auxin transport-feedback patterning mechanisms and is essential for organ initiation in the *Arabidopsis* inflorescence meristem (Heisler et al., 2005; Okada et al., 1991; Reinhardt et al., 2000; Reinhardt et al., 2003). However, in the vegetative state, the *pin1* mutant meristem still produces leaves positioned in a nonrandom order (Guenot et al., 2012). Therefore, PIN1-independent mechanisms must be involved, for instance, based on other PINs, auxin importers of the AUX1/LAX family, or transport-independent mechanisms. AUX1 and LAX1 are expressed predominantly in the L1, LAX2 is expressed in the incipient midvein, and LAX3 is not expressed in the meristem (Bainbridge et al., 2008; Heisler and Jönsson, 2006; Yadav et al., 2009). Phyllotactic patterning is disrupted in the triple *aux1 lax1 lax2* mutants under short days (Bainbridge et al., 2008). L1-expressed auxin influx carriers have been proposed to play a role in auxin retention in the surface layer (Heisler and Jönsson, 2006; Reinhardt et al., 2003). However, experimental data suggest that these proteins serve to maintain auxin gradients within the L1 itself, which would otherwise be lost due to apoplastic diffusion (Bainbridge et al., 2008). The vein-specific LAX2 may also play a role in organ positioning (Bainbridge et al., 2008).

It appears that correct lateral organ positioning requires the spatial and temporal coordination of multiple auxin transporters within the meristem, both influx and efflux. Although phyllotactic patterning is thought to occur primarily in the L1, it is tightly linked to midvein formation in inner tissue and shares the same auxin transport machinery. Coordination of multiple auxin transporters is required to create gradients in both the L1 and inner layers, as well as to regulate the movement of auxin between the layers. In the leaf, expression of PIN1 exclusively in the epidermis is sufficient for normal venation, which is thought to be due to redundancy with other plasma-membrane-localized members of the PIN family (Bilsborough et al., 2011). Here, we explore PIN1 function in the *Arabidopsis* inflorescence meristem by using tissue layer-specific expression and knockout of PIN1 in different auxin transporter mutant backgrounds. We show that PIN1 expression in the L1 is sufficient and necessary for regular phyllotaxis including midvein formation. Our data argue against the involvement of redundant plasma-membrane-localized PINs. Instead, PIN1 expression in inner tissues becomes indispensable when the L1-based auxin influx carriers are absent.

RESULTS

PIN1 Expression in the L1 Is Sufficient for Regular Phyllotaxis

The central and best characterized auxin transport regulator is PIN1. In order to test whether PIN1 expression in the L1 only is sufficient to restore phyllotaxis, we expressed a functional PIN1:GFP fusion under the control of the L1-specific ML1 promoter (Sessions et al., 1999) in the *pin1* mutant background. Thirty independent transformation lines were generated and checked for L1-specific expression. Seventeen of 30 independent transformants had no or very weak expression of PIN1:GFP in the meristem, and nine displayed aberrant expression (Figures S1A–S1F available online). Four lines exhibited L1-restricted PIN1:GFP signal and were selected for all further analysis (Figures 1A and 1B). When expressed from its own promoter, PIN1:GFP was found in the L1 as well as in the subepidermal layers, prominently in developing prevascular tissue (Figures 1C and 1D). When expressed from the ML1 promoter, PIN1:GFP corrected all *pin1* defects (Figures 1E and 1F). Organ morphology and fertility of these plants were indistinguishable from the control pPIN1::PIN1:GFP/*pin1* plants as well as from the wild-type (Figures 1E–1J). Detailed analysis of divergence angles between consecutive flower primordia revealed a restoration of wild-type organ positioning in the *pin1* mutant complemented with pPIN1::PIN1:GFP or pML1::PIN1:GFP constructs (Figures 1M–1O). These data point to a crucial role of PIN1 in the L1 for organ positioning.

PIN1 expression is known to be auxin inducible (Heisler et al., 2005). PLT-mediated upregulation of PIN1 expression in incipient primordia was suggested to be important for proper organ positioning (Prasad et al., 2011). However, recent data from the same group show that PLT-dependent PIN1 expression does not directly contribute to phyllotaxis (Pinon et al., 2013). Therefore, we quantified the green fluorescent protein (GFP) signal from the L1 layer for each individual L1 cell on eight to ten meristems of pML1::PIN1:GFP/*pin1* and control pPIN1::PIN1:GFP/*pin1* transgenic lines (Figures S1G–S1K). In control plants, we observed approximately 2.5-fold differences in the GFP signal intensity between cells with stronger GFP signal corresponding to the incipient and the most recently initiated primordia, I1 and P1 (Figure S1J). In the pML1::PIN1:GFP/*pin1* transgenic line, the overall GFP fluorescence was nearly two times higher than in the pPIN1::PIN1:GFP/*pin1* line ($1.8 \pm 0.4 \times 10^4$ and $1 \pm 0.4 \times 10^4$ arbitrary fluorescence units, respectively, $p < 0.001$; Figure S1K) but almost uniform within the peripheral zone (Figure S1I). Together, these data show that upregulation of PIN1 expression is dispensable for correct organ positioning. Therefore, phyllotactic patterning relies primarily on feedback of auxin on PIN1 polarization rather than on auxin-mediated transcriptional regulation, at least when overall PIN1 expression is high. Moreover, while the system is highly sensitive to reduction of PIN1 protein levels (Prasad et al., 2011) (Figures S1A–S1E), it appears tolerant of 2-fold PIN1 overexpression.

PIN1 in the L1 Is Necessary for Regular Organ Patterning

In order to determine whether PIN1 expression in the L1 is necessary for correct phyllotaxis, we specifically removed PIN1 activity from the L1 by Cre-loxP-mediated recombination. For this purpose, we made use of a two-component system (Adamski et al., 2009; Eriksson et al., 2010) (Figures S2M–S2O). One component consists of a PIN1:GFP gene flanked by loxP sites and driven by the cognate PIN1 promoter (Figure S2M). Expression of this construct in the background of the *pin1* mutant fully restores the wild-type phenotype (Figures 2A and 2E; Figures S2A, S2F, and S2K). The second component consists of an ethanol-inducible Cre recombinase gene driven by the ML1 promoter (Figure S2O). Deletion of the loxP-flanked fragment will result in cell-autonomous knockout of the PIN1:GFP gene (Figure S2N).

Removal of PIN1 from the L1 resulted in phyllotactic defects of different severity. In 45% of the observed meristems (49/108), organ initiation stopped after recombination, resulting in a pin-like phenotype (Figures 2B and 2F; Figures S2B and S2G). In 55% of the meristems (59/108), flower primordia continued to

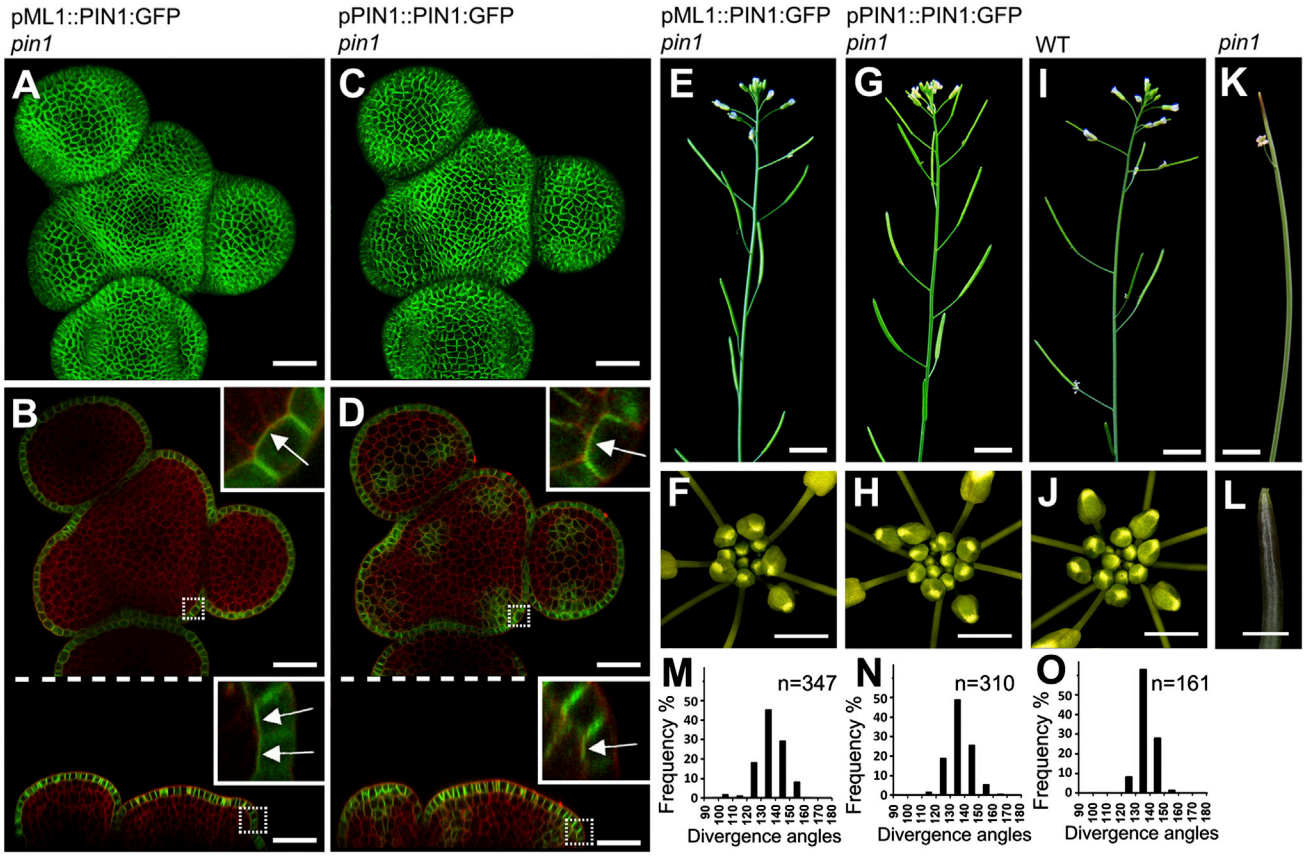

Figure 1. PIN1 Expression in the L1 Is Sufficient to Restore Normal Organ Formation and Phyllotactic Patterning in the *pin1* Mutant

(A–D) Expression pattern of pML1::PIN1:GFP, in (A) and (B), and pPIN1::PIN1:GFP, in (C) and (D), in the meristem of the *pin1* mutant. Maximal projections in (A) and (C); transversal sections 25 μm below the tip of the meristem in (B) and (D), top panels; and longitudinal sections in (B) and (D), bottom panels, from confocal stacks are shown. Cell wall stain: propidium iodide (PI) is indicated in red; GFP, in green. Insets: close-up view of L1 cells in recently initiated primordium. Dotted lines show positions of insets in samples. Arrows indicate PIN1 polarization in the L1 cells toward inner tissue.

(E–L) Phenotype of *pin1* mutant complemented with pML1::PIN1:GFP, shown in (E) and (F), or pPIN1::PIN1:GFP, shown in (G) and (H), compared to the wild-type, shown in (I) and (J), and *pin1* mutant, shown in (K and L).

(M–O) Divergence angles analysis for *pin1* mutant complemented with pML1::PIN1:GFP (M) or pPIN1:PIN1:GFP (N) compared to the wild-type (O). Total number of angles measured (n) is shown on each graph.

Scale bars, 30 μm (A–D); 1 cm (E, G, I, and K) and 2 mm (F, H, J, and L). See also Figure S1.

be initiated after PIN1:GFP removal from the L1 (Figures 2C and 2G). These primordia developed into flowers that were always abnormal, including a complete loss of fertility (Figure 2C; Figures S2B–S2E and S2L). Divergence angles between consecutive primordia were extremely variable compared to control (Figures 2I and 2J). In all recombined plants, PIN1:GFP expression was completely absent from the L1 (Figures 2F and 2G; Figures S2G–S2J). In the meristems that continued to initiate aberrant organs, areas of increased PIN1:GFP expression in the inner tissue corresponding to newly emerging primordia were observed (Figure 2G, arrowhead). We also noticed that the PIN1:GFP in the L2 layer of L1-recombined primordia tended to be localized on the membrane facing the L1 cell layer (Figure 2G, inset) or on the upper side of the membrane of anticlinal walls (Figure 2F, inset; Figures 2G, 2L, and 2M), suggesting that auxin may be transported from the inner tissue toward the L1. Therefore, we hypothesize that compensatory PIN1 expression in the inner tissue can partially substitute for the absence of PIN1 in the L1. In some cases, recombination resulted in specific PIN1:GFP knockout in both the L1 and L2 layers (Figures 2D and 2H). In contrast to the specific L1 knockout, these plants were characterized by a complete cessation of new organ initiation (100%, n = 10) (Figures 2D and 2H).

In order to determine auxin distribution in the periclinal chimeric plants, we crossed the auxin reporter line pDR5::3xVENUS-N7 (Brunoud et al., 2012; Heisler et al., 2005) into our pML1-Alc-Cre/PIN1:GFP/*pin1* line. In all nonrecombined control meristems, DR5 signal was detected mainly in groups of L1 cells corresponding to incipient and growing primordia as well as inner tissue cells located directly below (n = eight meristems) (Figure 2K). This DR5 expression pattern was similar to the one observed in the wild-type (n = 15 meristems) (Figure S3). L1-specific PIN1:GFP knockout resulted in relatively strong DR5 signal in 5 of 12 pin-like meristems (Figure 2L) and in 13 of 15 of the organ-initiating samples (Figure 2M). The correlation between DR5 accumulation and the position of

incipient or growing primordia was less obvious than for nonrecombined plants (Figure 2M). However, most of the DR5 signal was still localized in the L1 layer (Figures 2L and 2M). In contrast, in three samples recombined in both the L1 and L2 layers, the DR5 signal was always very weak or absent in the meristem (Figure 2N).

Taken together, these experiments show the crucial importance of the L1 for correct phyllotactic patterning. Surprisingly, they also suggest that when PIN1 is absent from the L1, PIN1 expressed in the L2 may, to some extent, compensate for the lack of PIN1 in the L1. This compensation allows for organ initiation, but positioning is aberrant.

The Midvein Develops Normally in the Absence of PIN1 in Inner Tissue

One of the first events in the venation process is the repolarization of PIN1 in the convergence point of the L1 from the anticlinal to the periclinal walls pointing toward inner tissue, enabling auxin to be transported locally from the L1 accumulation points to the inner tissue (Bayer et al., 2009; Scarpella et al., 2006). In order to verify if auxin is still actively transported into future veins in the absence of PIN1 expression in internal tissue, we first looked at the polarization of PIN1:GFP in the L1 of pML1::PIN1:GFP/*pin1* transgenic plants. In newly formed primordia of this line, PIN1 was polarized toward the inner tissue (Figure 1B, insets). The repolarization of PIN1 was also observed in pPIN1::PIN1:GFP/*pin1* control lines (Figure 1D, insets). This suggests that auxin can still be transported from the L1 surface layer toward inner tissue, even in the absence of PIN1 expression in the inner tissue.

To confirm auxin transport from the convergence point in the L1 to the inner tissue, we crossed pPIN1::PIN1:GFP/*pin1* and pML1::PIN1:GFP/*pin1* lines with plants expressing pDR5::3xVENUS-N7. In both lines, DR5 displayed a pattern of expression similar to that of the wild-type (compare Figures 3A and 3B with Figure S3). Auxin convergence points were localized at the initiation sites of new flower and sepal primordia. In both lines, we observed localized expression of DR5 outside the L1, strongly suggesting that auxin is transported from the L1 toward inner tissue (Figures 3A and 3B, arrows and insets). Since the DR5 reporter is also one of the earliest molecular markers of prevasculature development (Scarpella et al., 2006), it suggests that vein positioning and development are normal in both lines.

We crossed prevasculature markers pLAX2::GUS (Bainbridge et al., 2008) and pATHB8::GUS (Baima et al., 1995) into our transgenic lines. For both markers, GUS staining was detected in the same tissues independent of whether PIN1 was expressed from pML1 or its own promoter (Figures 3C–3F). Furthermore, later developmental stages showed normal vascular traces in both lines (Figures 3G and 3H), confirming that vascular development proceeds normally with or without PIN1 in internal tissue. This is consistent with previous experiments showing a restoration of wild-type leaf serration and leaf venation in *pin1* mutants by pML1::PIN1:GFP (Bilsborough et al., 2011). Taken together, these data suggest that L1-specific PIN1 expression is sufficient for organ initiation, correct positioning, and proper vein patterning followed by normal organ outgrowth.

No Function for Other Plasma-Membrane-Localized PINs or the Putative Auxin Importer LAX2

In addition to PIN1, four other plasma-membrane-localized PIN proteins are encoded in the *Arabidopsis* genome (PIN2, PIN3, PIN4, and PIN7) (Paponov et al., 2005). None of them is expressed in the shoot apical meristem itself, neither in wild-type nor in *pin1* mutant backgrounds (Guenot et al., 2012). Furthermore, single knockout mutations in genes coding for other members of the PIN family have no effect on phyllotactic patterning in the inflorescence shoot apex (Figures 4A, 4D, 4G, and 4J). Nevertheless, the compensatory action of other PINs in the absence of PIN1 activity in the inner tissue cannot be excluded. Such an ectopic expression of other PINs has previously been observed in roots (Blilou et al., 2005; Vieten et al., 2005). To test this hypothesis, we crossed *pin2*, *pin3*, *pin4*, and *pin7* mutations into the pPIN1::PIN1:GFP/*pin1* and pML1::PIN1:GFP/*pin1* transgenic lines. Inflorescence phenotypes of *pin1/pin2*, *pin1/pin3*, *pin1/pin4*, *pin1/pin7* double mutants and *pin1* single mutants expressing either transgene were comparable to wild-type, with the distributions of divergence angles centered around the theoretical value of 137° (Figures 4A–4L). These data, together with previously published results (Guenot et al., 2012), argue against a role of the other plasma-membrane-localized PINs in the meristem's inner tissue.

Since mutations in the plasma-membrane-localized PINs have no discernible effects on organ positioning, we wondered whether non-PIN auxin transporters might be involved in vein formation. The *Arabidopsis* genome encodes a family of four auxin influx carriers (Parry et al., 2001). LAX2 is the only member of the family to be expressed specifically in the prevascular tissue of the meristem (Bainbridge et al., 2008) (Figures 3C and 3D). The *lax2* single mutant has a mild vein development defect in the cotyledons (Péret et al., 2012) but displays normal phyllotaxis (Figure 4M). Additionally, mutating this gene increased the mild phyllotaxis phenotype of the *aux1/ lax1* mutant (Bainbridge et al., 2008). For these reasons, LAX2 might function in developing veins to increase auxin sink strength, draining auxin from the L1. To test this hypothesis, we expressed pML1::PIN1:GFP and pPIN1::PIN1:GFP constructs in the *pin1/lax2* double mutant background. Both transgenes were able to rescue the phenotype of *pin1/lax2* double mutants to wild-type (Figures 4N and 4O). Thus, despite its suggestive expression pattern, LAX2 is dispensable for organ positioning and, presumably, also for vein initiation in meristems without PIN1 expression in the inner tissue.

L1-Expressed AUX1 and LAX1 Influx Carriers Compensate for Lack of PIN1 in Internal Tissue

Two other members of the auxin influx carrier family, AUX1 and LAX1, have overlapping expression in the L1 surface layer of the apex (Bainbridge et al., 2008; Heisler and Jönsson, 2006; Yadav et al., 2009). We asked whether L1-specific PIN1 phenotypic rescue requires the presence of the L1-specific influx carriers. To answer this question, we introduced the pPIN1::PIN1:GFP and pML1::PIN1:GFP constructs into different combinations of *pin1*, *aux1*, and *lax1* mutant backgrounds (Figure 5; Figure S4).

Under long day conditions, the *aux1* or *lax1* single mutants display normal phyllotaxis (Bainbridge et al., 2008) (Figure S4A

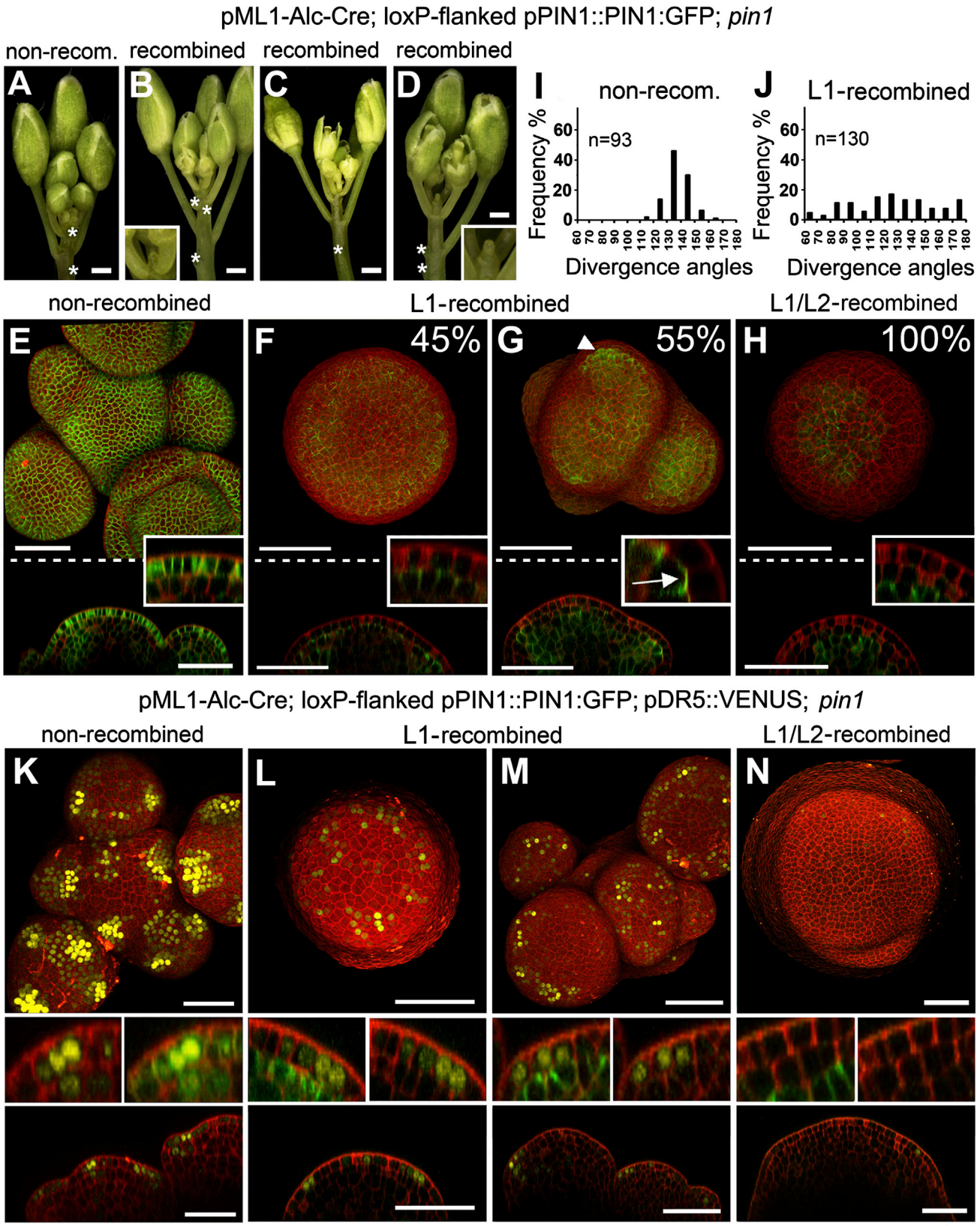

(legend on next page)

and S4D). pML1::PIN1:GFP and pPIN1::PIN1:GFP constructs were able to restore correct organ positioning in the *pin1* mutant in the absence of either AUX1 or LAX1 (Figures S4B, S4C, S4E, and S4F), indicating that these two proteins have redundant functions in the meristem. In agreement with previous work (Bainbridge et al., 2008), the *aux1/lax1* double mutant displays a mild phyllotaxis phenotype with organ-positioning defects in only some individuals (7/42 = 17% abnormal) (Figures 5A and 5B). Expression of pPIN1::PIN1:GFP in the *pin1/aux1/lax1* background restored organ formation and positioning comparable to that of the *aux1/lax1* double mutant (34/93 = 37% abnormal) (Figures 5C and 5D). The distributions of divergence angles in both lines were centered around the theoretical value of 137°, typical for wild-type spiral phyllotaxis with slightly higher variability for the PIN1:GFP-expressing line (Figures 5G and 5H). In both groups, we observed similar, relatively rare defects in floral organ number (Figures 5A and 5C, arrows).

In contrast, when pML1::PIN1:GFP was expressed in the same *pin1/aux1/lax1* background, the plants were clearly abnormal (Figures 5E and 5F). In 39 of 131 observed meristems, organ initiation was transiently arrested (Figure 5F). When organs did form, their positioning was aberrant (85/131 = 64% abnormal) (Figure 5E; Figure S4J), except for a few meristems with phyllotaxis close to that of wild-type (7/131 = 5%). In those plants that formed organs, the distribution of divergence angles was very broad and clearly different from that of control *aux1/lax1* or pPIN1::PIN1GFP/*pin1/aux1/lax1* (compare Figures 5G–5I). Significant numbers of wide and fused flower primordia were observed (Figure 5E; Figure S4K). Flowers were defective, with abnormal numbers of organs (Figure 5E and 5F, arrows) and reduced fertility.

PIN1:GFP expression from the ML1 promoter is approximately two times stronger than that from PIN1 promoter (Figure S1K). This might increase auxin export and lower intracellular auxin levels. Could it be that the loss of the importers in combination with enhanced export activity decreases cellular auxin levels below a critical threshold? In the wild-type background, increasing PIN1 dosage by expressing PIN1:GFP either from the native or the ML1 promoter had no effect on organ positioning (Figures S4G–S4I). Similarly, both pPIN1::PIN:GFP/*aux1/lax1* and pML1::PIN1-GFP/*aux1/lax1* yielded phyllotactic patterns centered around 137° in the presence of an extra dosage of PIN1 (Figures S4L–S4Q). Moreover, in the pML1::PIN1:GFP/*pin1/aux1/lax1* plants, no significant differences in PIN1 expression were found between the 19 meristems that made organs versus the nine that were pin-like (15,000 ± 2,000 and 14,000 ± 1,000 arbitrary fluorescence units, respectively; $p = 0.175$). These data suggest that the strong phenotype of the pML1::PIN1:GFP/*pin1/aux1/lax1* line cannot be explained by PIN1 overexpression but is the cumulative result of the absences of importers in the L1 and PIN1 in the inner tissue.

PIN1 Aids Auxin Retention in the L1

Previous mathematical modeling suggested that the AUX1 import carrier has a key role in auxin retention in the L1 (Heisler and Jönsson, 2006); however, in *aux1/lax1/lax2* triple mutants, L1 auxin levels remain high (Bayer et al., 2009). During primordium initiation, PIN1 is initially oriented toward the L1 in inner layers, suggesting that PIN1 may help to retain auxin in the L1. This is consistent with gradient-based PIN polarization (Bayer et al., 2009; Jönsson et al., 2006; Smith et al., 2006) with inner tissue PINs polarization toward the higher auxin concentration cells in the L1. In this scenario, the absence of influx carriers in the L1 and lack of PIN1 in the inner tissue would result in auxin diffusion from the L1 to the layers below.

To test this hypothesis, we first checked whether PIN1 expression in the L2 is upregulated in the absence of AUX1 and LAX1 transporters. Because expression of PINs is auxin responsive (Benková et al., 2003; Blilou et al., 2005; Friml et al., 2003; Laskowski et al., 2006; Vieten et al., 2005), we reasoned that auxin diffusing from the L1 would induce PIN1 expression in the inner tissue. Indeed we noticed that the expression of PIN1:GFP from its own promoter was clearly increased within the L2 in the absence of AUX1 and LAX1 (Figures 6A and 6B). Relative GFP signal in the L2 layer was more than 50% higher in the *pin1/aux1/lax1* triple mutant, compared to a *pin1* single mutant background (26% ± 4% and 17% ± 3% relative to expression in the L1 respectively, $p < 0.001$) (Figure 6E). In contrast, the expression of PIN1:GFP from the ML1 promoter in the L2 layer was very low and stable, independent of the mutant background (Figures 6C–6E).

Figure 2. PIN1 Knockout in L1 Abolishes Phyllotactic Patterning

(A–D) Phenotype of *pin1* mutant carrying the loxP-flanked pPIN1::PIN1:GFP construct and the pML1-Alc-Cre transgene. In the absence of recombination (A), organ formation at the meristem is rescued by loxP-flanked transgene. After PIN1 knockout in the L1 organ initiation is abolished (B) resulting in a pin-like phenotype (inset in B), or impaired (C) with only abnormal flowers continuing to be produced at the meristem. When PIN1 was knocked out in both L1 and L2, organ initiation was stopped (inset in D). Asterisks indicate flowers removed for clarity.

(E–H) Expression patterns of PIN1:GFP in the meristems of the same plants as shown in (A) through (D). Without recombination, PIN1-GFP was detected mainly in the L1 and prevascular tissue (E). After L1-specific recombination, PIN1-GFP was absent in the L1, as shown in (F) and (G). In some plants, recombination resulted in PIN1 knockout both in the L1 and L2 (H). Arrows indicate PIN1:GFP polarization in L2 cells toward L1 in the recently initiated primordium. Upregulation of PIN1:GFP in the L2 in primordia was often observed (arrowhead).

(I and J) Divergence angles analysis of *pin1* mutants carrying the loxP-flanked pPIN1:PIN1:GFP construct and the pML1-Alc-Cre transgene. Total number of angles measured (n) is shown for each graph.

(K–N) Expression patterns of pDR5::3xVENUS-N7 in the meristem of *pin1* mutants carrying the loxP-flanked pPIN1:PIN1:GFP construct and the pML1-Alc-Cre. In nonrecombined plants (K), DR5 can be seen in flower and sepal primordia, similar to the wild-type plants. In L1-recombined, pin-like meristems (L), DR5 is present in the L1 in several dispersed cells. In L1-recombined meristems that continue to form organs (M), DR5 is still mainly detected in the L1 with less obvious accumulation points in primordia than in nonrecombined meristems. In L1/L2-recombined meristems, DR5 signal is very weak and localized in just few dispersed cells (N).

In (E) through (H) and (K) through (N), the maximal projection (top pictures) and longitudinal section (bottom pictures) from confocal stacks are shown. Insets show close-up views of the L1 and L2 cells. PI is indicated in red; GFP, in green; and VENUS, in yellow.

Scale bars, 2 mm (A–D) and 50 μm (E–H and K–N). See also Figure S2 and S3.

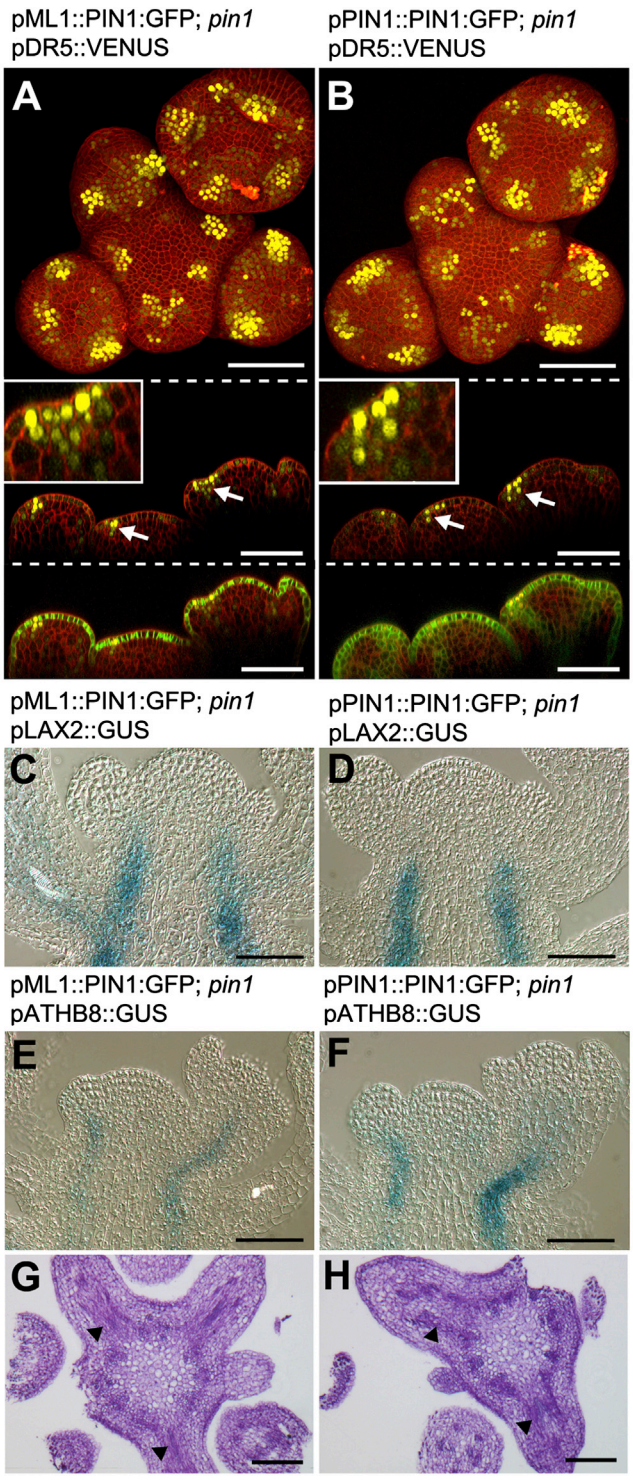

Figure 3. Vein Specification Is Unaffected in Plants Expressing PIN1 Only in the L1

(A and B) Expression pattern of pDR5::3xVENUS-N7 in meristems of *pin1* mutant complemented with pML1::PIN1:GFP (A) or pPIN1::PIN1:GFP (B). Maximal projections (top panels) and longitudinal sections (middle and bottom panels) of confocal stack are shown. Insets show close-up view of DR5 signal in recently initiated primordia. PI is indicated in red, and YFP is indicated in yellow; GFP, in green, is shown only in the bottom panels.

(C and D) Expression pattern of pLAX2::GUS in *pin1* mutant complemented with pML1::PIN1:GFP (C) or pPIN1::PIN1:GFP (D). Histological GUS staining of median longitudinal sections through inflorescence meristems is shown.

(E and F) Expression pattern of pATHB8::GUS in *pin1* mutant complemented with pML1::PIN1:GFP (E) or pPIN1::PIN1:GFP (F). Histological GUS staining of median longitudinal sections through inflorescence meristems is shown.

(G and H) Vascular patterning in the *pin1* mutant complemented with pML1::PIN1:GFP, section 240 μm below the meristem tip (G), or pPIN1::PIN1:GFP, section 232 μm below the tip (H). Oblique sections showing vascular traces are shown. Arrowheads indicate xylem strands.

Scale bars, 50 μm (A–F) and 100 μm (G and H). See also Figure S3.

Finally, to assess more directly the importance of PIN1 expression in internal tissue for auxin retention in the L1, we monitored the auxin activity marker DR5 in our transgenic lines. In 79% of *pin1/aux1/lax1* mutant meristems expressing PIN1 from its own promoter (19/24), DR5 signal was detected mainly in the groups of L1 cells corresponding to incipient and growing primordia and in inner tissue cells located below (Figure 6F). Weak DR5 signal was often detected in the L1 of the cells located between primordia (Figure 6F). In the remaining 21% of meristems of this line, DR5 signal was weak, with occasionally only a few cells expressing DR5 (data not shown). Strikingly, in the pML1::PIN1:GFP/*pin1/aux1/lax1* line, DR5 signal was, most of the time, absent (53/68 = 78%) or very weak (15/68 = 22%) in the meristems themselves and in incipient primordia (Figures 6G and 6H). DR5 convergence points in the L1 and its internal tissue localization were observed in most samples of this line, almost exclusively in sepal primordia (Figure 6G).

All together, these data strongly indicate that L1 expressed AUX1 and LAX1 together with PIN1 expressed in the inner tissue function in auxin retention in the L1. This demonstrates the importance of a fine balance between auxin influx and efflux at the tissue level for proper organ initiation and positioning.

DISCUSSION

Organ initiation at the shoot apical meristem involves two auxin-dependent processes: the formation of an auxin maximum in the L1 and patterning of a line of high auxin cells extending from the L1 into the internal cell layers and eventually connecting with older leaf traces. Both processes are accompanied by highly stereotypic patterns of PIN1 expression and subcellular localization (Bayer et al., 2009; Heisler et al., 2005; Reinhardt et al., 2003; Scarpella et al., 2006). We explored the interdependency between these processes by using tissue layer-specific expression and knockout of PIN1 in different auxin transporter mutant backgrounds (for a graphical summary, see Figure 7). When PIN1 was exclusively expressed in the L1, organ formation and positioning were normal, and the auxin reporter DR5, as well as the early midvein markers LAX2 and ATHB8, were expressed as they are in wild-type plants (Figures 1 and 3). Conversely, removing PIN1 specifically from the L1 layer severely affected both organ initiation and positioning (Figure 2). Thus, expression of PIN1 in the L1 is sufficient and necessary for correct organ positioning and midvein patterning (Figures 7A, 7B, and 7E). This lends strong credibility to mathematical models of phyllotaxis that exclusively consider L1-based patterning processes (de Reuille et al., 2006; Jönsson et al., 2006; Smith et al., 2006; Stoma et al., 2008).

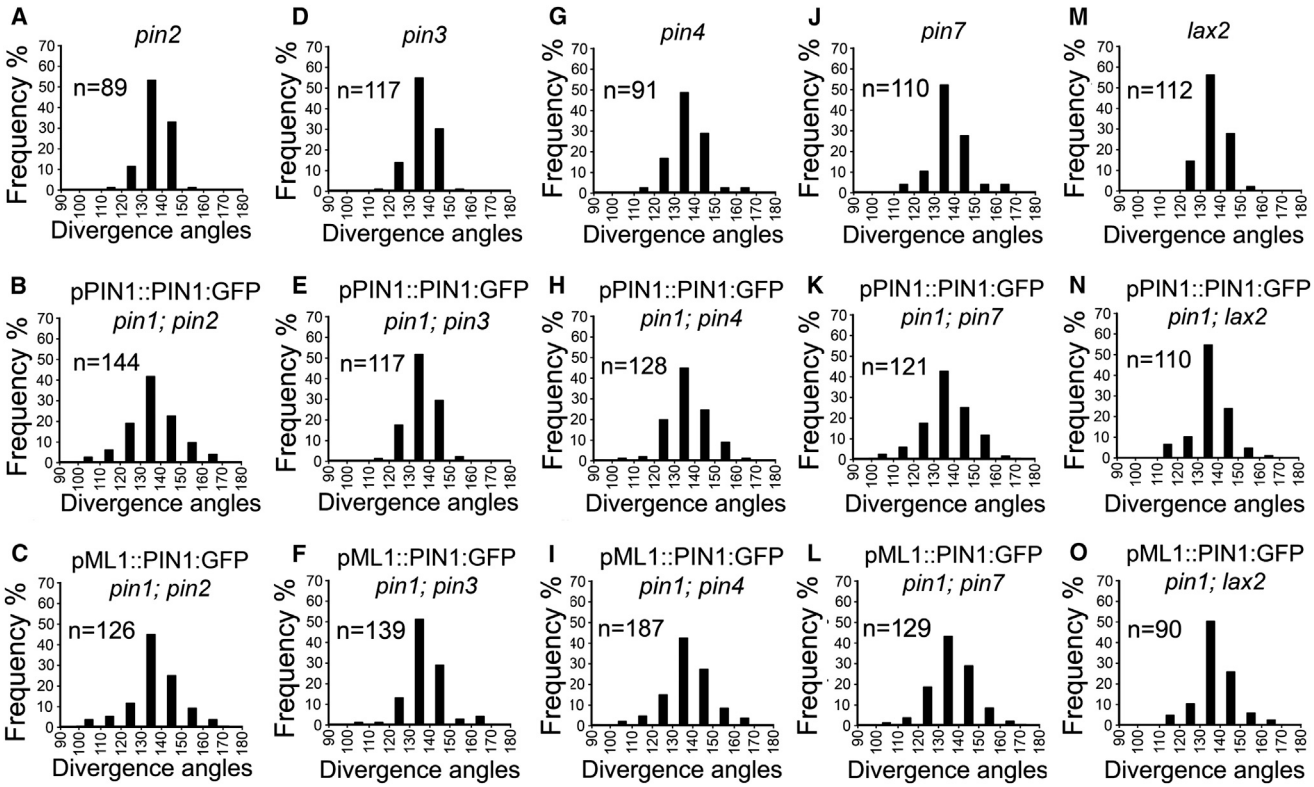

Figure 4. No Function for Other Plasma-Membrane-Localized PINs or the Putative Auxin Importer LAX2

(A–C) Distribution of divergence angles of *pin2* single mutant (A) compared to *pin1/pin2* double mutant complemented with pPIN1::PIN1:GFP (B) or pML1::PIN1:GFP (C).

(D–F) Distribution of divergence angles of *pin3* single mutant (D) compared to *pin1/pin3* double mutant complemented with pPIN1::PIN1:GFP (E) or pML1::PIN1:GFP (F).

(G–I) Distribution of divergence angles of *pin4* single mutant (G) compared to *pin1/pin4* double mutant complemented with pPIN1::PIN1:GFP (H) or pML1::PIN1:GFP (I).

(J–L) Distribution of divergence angles of *pin7* single mutant (J) compared to *pin1/pin7* double mutant complemented with pPIN1::PIN1:GFP (K) or pML1::PIN1:GFP (L).

(M–O) Distribution of divergence angles of *lax1* single mutant (M) compared to *pin1/lax1* double mutant complemented with pPIN1::PIN1:GFP (N) or pML1::PIN1:GFP (O).

Total number of angles measured (n) is shown on each graph.

Unexpectedly, we found that the L1-expressed auxin influx carriers, AUX1 and LAX1, become indispensable for correct organogenesis when PIN1 is expressed from the ML1 promoter (Figure 5). At the molecular level, the most striking observation is the virtual absence of DR5 expression in the meristem of the pML1::PIN1:GFP/*pin1/aux1/lax1* line, compared to the control (Figure 6). Thus, only the broader PIN1 expression from its native promoter can compensate for the loss of AUX1/LAX1 activity, and curiously, correct organ initiation and positioning require either auxin import activity in the L1 or PIN1-driven auxin export activity below the L1. How is it that these spatially separated and functionally distinct auxin transporters have some redundancy, with either being required for normal DR5 expression and organogenesis? The opposite actions of exporters and importers are relevant here. PIN1 facilitates auxin export into the extracellular space where auxin can move between cells but is unavailable to the genetic auxin response machinery. In contrast, the importers retain auxin within cells, where it will activate its receptors. The balance between auxin export and auxin retention can explain several interactions between tissue layers. First, in the absence of AUX1/LAX1 activity, PIN1 is ectopically expressed in the L2 (Figure 6). We suggest that, without the importers, more auxin diffuses into the L2, inducing PIN1 gene expression. Second, PIN1 knockout in both the L1 and the L2 completely abolishes organogenesis, whereas knockout of PIN1 exclusively in the L1 interferes with organogenesis but only partially abolishes it (Figure 2). This indicates that PIN1-based auxin transport in the L2 can partially rescue organ initiation but not well enough for reliable positioning. Third, in plants with specific PIN1 knockout in the L1 that continue to form organs, PIN1 in the L2 tends to polarize toward the L1, and considerable DR5 expression is observed within the L1 (Figure 2). Therefore, PIN1 expression below the L1 can enhance DR5 convergence points in the L1.

In the classical scenario, an auxin maximum in the L1 is created through a positive feedback between auxin and

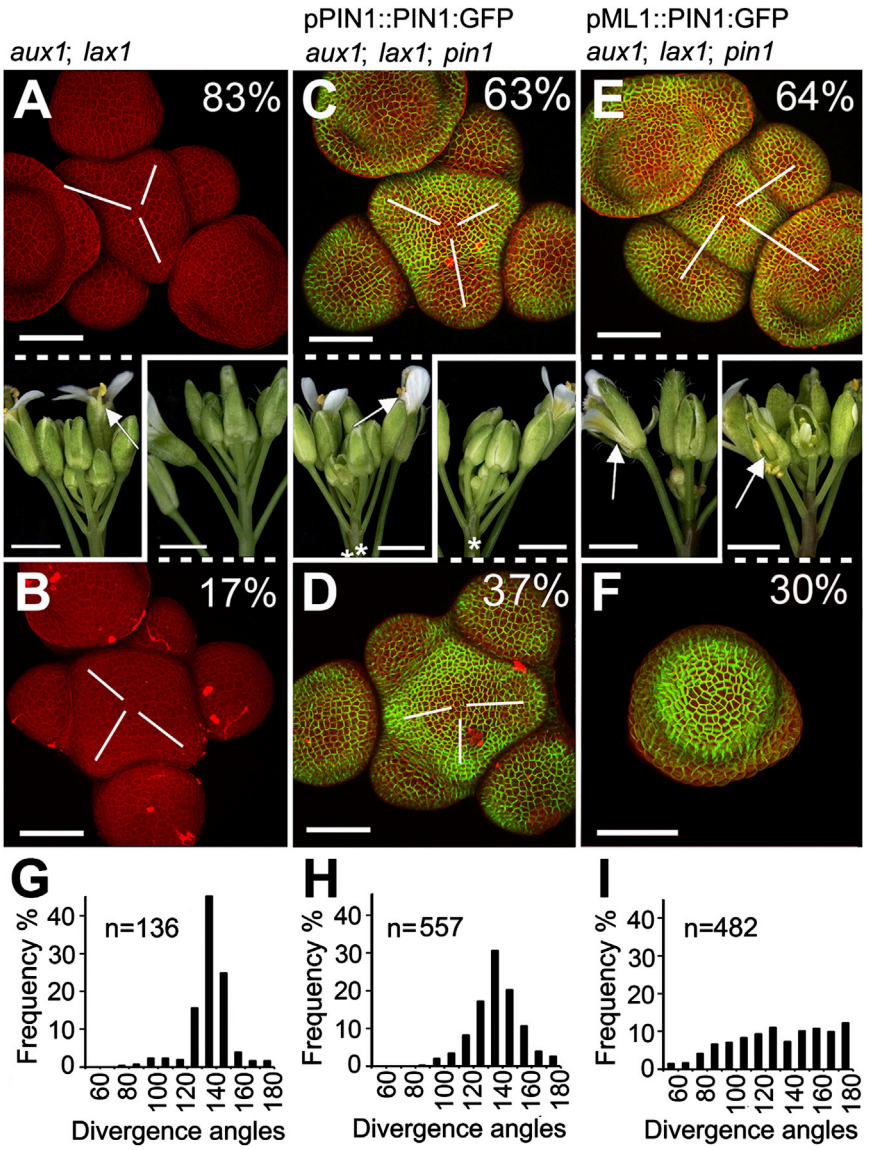

Figure 5. PIN1 Expression in the L1 Is Sufficient to Restore Normal Phyllotaxis Only in the Presence of L1-Localized Influx Carriers

(A–F) Inflorescence phenotype of different lines lacking L1 expressed AUX1 and LAX1 influx carriers. Maximal projections of confocal stacks and light images of the same representative samples are shown. PI is shown in red; GFP, in green. Arrows indicate missing floral organs. White lines indicate divergence angles between successive primordia. (A) and (B) show the *aux1/lax1* double mutant. In most of the samples (35/42), the phyllotaxis was normal, as shown in (A). Slight defects were observed in eight plants, as shown in (B). (C) and (D) show the *aux1/lax1/pin1* triple mutant complemented with pPIN1::PIN1:GFP. In most of the cases (59/93) phyllotaxis was normal, as shown in (C). Defects in organ positioning were observed in 34/93 meristems, as shown in (D). (E) and (F) show the *aux1/lax1/pin1* triple mutant complemented with pML1::PIN1:GFP. Most of samples displayed abnormal organ positioning (85/131), as shown in (E), or cessation of new organ formation (39/131), as shown in (F). Flower primordia were often enlarged, as shown in (E).

(G–I) Distribution of divergence angles of the transgenic lines shown in (A) through (F). Total number of angles measured (n) are shown on each graph.

Scale bars, 50 μm (confocal images) and 2 mm (light images). See also Figure S4.

up-the-gradient PIN1 polarization (Jönsson et al., 2006; Smith et al., 2006). The auxin maximum then induces PIN1 expression and vein specification in the inner tissues by polarizing PIN1 with the flux (Bayer et al., 2009; Mitchison, 1980; Rolland-Lagan and Prusinkiewicz, 2005; Stoma et al., 2008). The data presented here show that, in the presence of AUX1 and LAX1, PIN1 is dispensable in inner tissues. We suggest that the auxin maximum in the L1 is enhanced through retention of auxin by AUX1 and LAX1 and that, under these conditions, vein specification appears to proceed by a PIN1-independent mechanism. In the absence of the two importers, the auxin maximum in the L1 will be less pronounced, and vein specification becomes dependent on PIN1 in inner tissues. It appears that convergence point formation in the L1 critically depends on cell-autonomous expression of PIN1 but that vein formation persists without PIN1 expression in internal cell layers. Thus, the two processes can be genetically separated, suggesting that they involve distinct mechanisms.

The first sign of specification of future vascular cells is the expression of PIN1 (Bayer et al., 2009; Scarpella et al., 2006). It comes as a surprise that, despite being expressed in intricate and highly suggestive cellular and subcellular patterns, PIN1 can be dispensable in future vein cells. What then causes patterning in the inner tissues? No other plasma-membrane-localized members of the PIN family could substitute for PIN1 in phyllotaxis patterning (Figure 4) (Guenot et al., 2012). Based on its expression pattern, its phenotype in cotyledons, and mathematical modeling, the LAX2 importer seemed a plausible candidate (Bainbridge et al., 2008; Kramer, 2004; Péret et al., 2012). However, the elimination of LAX2 function did not affect organ positioning and midvein formation (Figure 4). Mitchison (1980) proposed two models of canalization, one based on polar transport and one based on facilitated diffusion. Although largely dismissed since the discovery of polarized PINs in vein precursor cells, the facilitated diffusion mechanism is more robust, does not create cycles, and can more directly find sink tissues below (Smith and Bayer, 2009). In his original papers, Mitchison suggested that enhanced flux might become canalized by local induction of plasmodesmata (Mitchison, 1980). A more up-to-date possibility is the upregulation of apolar transporters, which could act to make vein precursor cells more diffusive to auxin. Facilitated diffusion can work robustly with any type of auxin transporter,

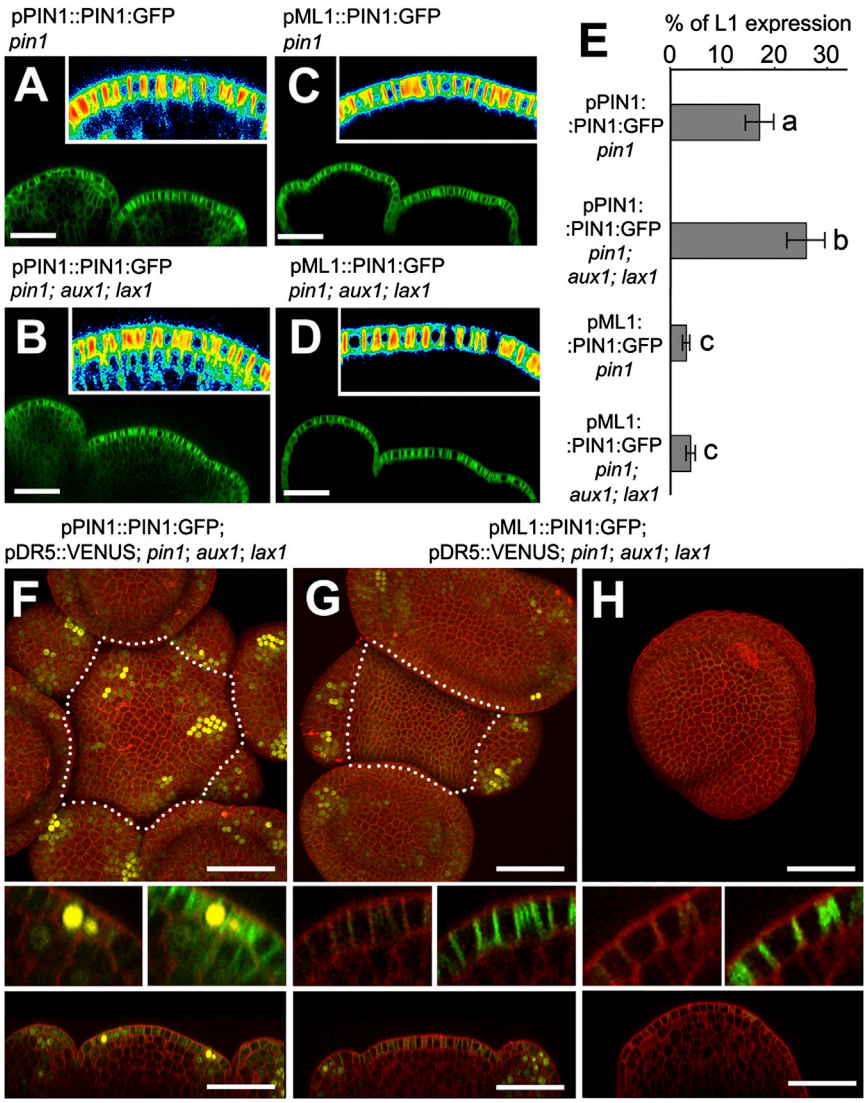

Figure 6. PIN1 in the Inner Tissue Aids Auxin Retention in the L1

(A–D) Expression pattern of pPIN1::PIN1:GFP, in (A) and (B), or pML1::PIN1:GFP, in (C) and (D), in *pin1* single mutant background, in (A) and (C), or *pin1/aux1/lax1* triple mutant background, in (B) and (D). Longitudinal sections through confocal stacks are shown. Insets show pseudocolored images of PIN1:GFP signal intensity in the center of the meristem. Signal intensities are displayed in blue to red corresponding to increasing intensity levels. Note a relative increase of GFP signal in the L2 cell layer in the *pin1/aux1/lax1* triple mutant (B) compared to single *pin1* mutant (A) in pPIN1::PIN1:GFP-expressing lines (26% ± 4% and 17% ± 3%, respectively; n = ten meristems, p = 0.0004). This increase was not detected when PIN1:GFP was expressed from the ML1 promoter, as shown in (C) and (D) (3% ± 1% and 4% ± 1% for *pin1* and *pin1/aux1/lax1*, respectively; n = 10 meristems, p = 0.08).

(E) Quantification of relative GFP signal in the meristem L2 layer of *pin1* or *pin1/aux1/lax1* mutants complemented with pPIN1:PIN1:GFP or pML1::PIN1:GFP. Fluorescence signal in the L2 is presented as a fraction of the L1 signal. Error bars indicate SD (n = 10–11 meristems). Different letters for each value indicate statistically significant differences in Mann-Whitney U test ($p < 0.05$).

(F–H) Expression pattern of pDR5::3xVENUS-N7 in meristems of *pin1/aux1/lax1* triple mutant complemented with pPIN1::PIN1:GFP (F) or pML1::PIN1:GFP, shown in (G) and (H). Maximal projections (top panels) and longitudinal sections (bottom panels) of confocal stacks are shown. In pPIN1::PIN1:GFP lines, DR5 signal is present in the meristem in incipient primordia (F). Insets show close-up views of periphery of the meristem. PI in red; VENUS in yellow; GFP in green is shown only in right insets.

Scale bars, 50 μm.

importers or exporters, located inside the cells or at the plasma membrane (Mitchison, 1980; Rolland-Lagan and Prusinkiewicz, 2005). These include endoplasmic-reticulum-localized PINs, the newly reported class of PIN-like proteins, ATP-binding cassette transporters (Barbez et al., 2012; Ding et al., 2012; Friml and Jones, 2010; Geisler et al., 2005; Mravec et al., 2008, 2009; Sawchuk et al., 2013), or as yet undiscovered transporters. Such a mechanism may also be relevant in the vegetative meristem that can position its organ nonrandomly in the absence of PIN1 or in the leaf that makes veins without PIN1 (Bilsborough et al., 2011; Guenot et al., 2012). It might also be relevant in the gametophyte of the moss *Physcomitrella patens*, in which no polar auxin transport could be detected (Fujita et al., 2008; Wabnik et al., 2011). It may be that the PIN1-polarization-based patterning mechanisms that have been intensely studied in flowering plants were preceded in evolution by an apolar mechanism for which a defined auxin source, a sink, and any type of broad-specificity carrier with affinity for auxin would suffice.

EXPERIMENTAL PROCEDURES

Plant Material

All *Arabidopsis thaliana* mutants and transgenic lines were in the standard Columbia background. Transgenes analyzed in mutant and wild-type backgrounds are listed in the Supplemental Experimental Procedures. Plants carrying more than one transgene were generated by crosses. F2/F3 progeny were screened for phenotypes and/or presence of fluorescent protein signal. For mutants, the homozygous plants were identified by phenotype, PCR genotyping, or antibiotic selection and segregation analysis. Primers used for genotyping are listed in the Supplemental Experimental Procedures. For mutant alleles, PCR products were shorter (approximately 500–700 base pairs [bp]), and for wild-type alleles, they were longer (approximately 900–1,500 bp). To detect the *aux1-21* mutant allele, the PCR product was digested using the ApaL1 restriction enzyme, resulting in 800 bp and 1,200 bp bands, while the wild-type allele was not digested by this enzyme. To detect *pin2* homozygotes, we screened plants for agravitropic response.

Plant Growth Conditions

Plants were grown on soil in a growth chamber under long day conditions (16 hr of illumination, 110 $\mu Em^{-2}s^{-1}$) at 20 ± 2°C, with 65% ± 10% relative

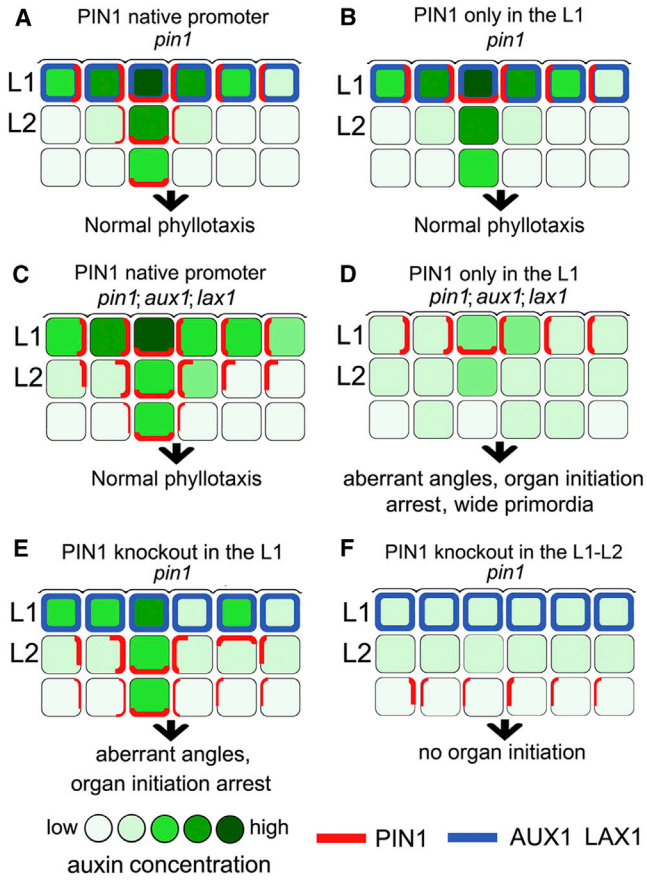

Figure 7. Summary of the Role of Layer-Specific Auxin Transporters in Phyllotaxis

Schematic representation of a longitudinal section through the shoot apical meristem. The auxin exporter PIN1 is assumed to be auxin inducible and to polarize toward cells with either higher auxin concentration or higher flux, as proposed by Bayer et al. (2009). AUX1 and LAX1 are expressed in the L1, are apolar, and promote the import of auxin into cells. Auxin concentration (green scale), PIN1 (red), and AUX1/LAX1 (blue) are shown.

(A) In the wild-type, auxin is transported mainly in the L1 layer, and through the combined action of PIN1 and AUX1/LAX1, strong local auxin maxima are formed. At these auxin convergence points, PIN1 acquires a basal polarization and pumps auxin into inner layers. Successive expression and basal/lateral polarization of PIN1 (Bayer et al., 2009) result in vein patterning. This highly controlled generation of auxin peaks and subsequent auxin draining toward inner tissue results in the generation of regular angles of 137° between successive primordia.

(B) When PIN1 is expressed from the pML1 promoter, transport of auxin and generation of convergence points take place in the L1. As in the wild-type situation, the combined action of PIN1, AUX1, and LAX1 produces normal convergence points. Once an auxin convergence point is formed, PIN1 in the L1 acquires basal polarization and pumps auxin locally into inner tissue. Vein patterning proceeds normally. We propose that this is due to the activity of other, as yet unidentified, auxin transporters. Despite the absence of PIN1 in inner tissues, phyllotaxis is normal.

(C) The absence of the importers causes more auxin diffusion into the L2 and less efficient convergence point formation in the L1. However, auxin-induced PIN1 expression and polarization in the L2 aids convergence point formation and subsequent PIN1-mediated canalization.

(D) In meristems expressing PIN1 only in the L1 and in the absence of AUX1 and LAX1, auxin exported by PIN1 cannot be efficiently taken up by the cells, and more auxin diffuses into inner tissue. Because of the lack of PIN1 in internal tissues, auxin cannot be transported back to the L1, and the overall auxin level in the L1 layer drops. This results in poor convergence point formation and severe phyllotactic aberrations.

(E) Knockout of PIN1 in the L1 can be partially compensated by ectopic expression in the L2, where it is polarized toward the L1. This PIN1 transports auxin locally toward the L1, generating rare and random auxin convergence points in the L1 that may be further amplified presumably by auxin influx carriers and/or local auxin synthesis. This, in turn, results in transient and irregular initiation of primordia.

(F) Knockout of PIN1 in both L1 and L2 results in dramatic decrease in DR5 expression completely abolishing organ formation.

humidity. For antibiotic selection, plants were grown on ½ Murashige & Skoog medium supplemented with 1% sucrose, 0.1% plant protective medium, and appropriate antibiotic.

PIN1:GFP knockout in the L1 was achieved by inducing pML1-Cre plants with ethanol vapor within sealed plastic bags for 5–15 min. The plants were observed 1–2 weeks after ethanol application, except for plants shown in Figure S2, which were observed after 3 weeks. In some cases, we observed a spontaneous recombination, which often resulted in complete and specific PIN1:GFP knockout in the L1.

Construction of Transgenes and Plant Transformation

Constructs for plant transformation were generated according to standard cloning techniques as described in the Supplemental Experimental Procedures. Plant transformation was performed using the floral dip method (Clough and Bent, 1998).

Histology and Microscopy

Histological sections were prepared and stained for β-glucuronidase expression as described elsewhere (Sessions et al., 1999). For staining of vasculature, tissues were fixed in 4% formaldehyde in PBS overnight and then embedded in paraplast. The 8 μm sections were stained for 20 min with 0.001% toluidine blue. Signal was observed with a Zeiss Axioskop 2 light microscope equipped with differential interference filters and a Zeiss AxioCam MRm digital camera.

The red fluorescent protein DsRED2 and cyan fluorescent protein (CFP) fluorescence in whole plants were observed with a modified Leica MZ12 dissecting microscope fitted with a Zeiss AxioCam MRm digital camera. Excitation was achieved using a 434/17 nm filter set for CFP and a 599/34 nm filter set for DsRED2. Fluorescence was captured using a 479/40 nm filter set for CFP and a 630/69 nm filter set for DsRED2.

Confocal imaging was carried out using a Leica upright confocal laser scanning microscope (Leica TCS SP5) with long-working-distance water immersion 63× or 20× objectives. Excitation was achieved with an Argon laser line at 488 nm (GFP and propidium iodide [PI]), 514 nm (VENUS), and 458 nm (CFP). Fluorescence was captured at 497–542 nm (GFP), 592–671 nm (PI), 535–600 (VENUS), and 465–496 nm (CFP). To visualize cell walls, we stained meristems with 0.1% PI (Sigma-Aldrich) for 2–5 min. Microscopic observations were performed 5–6 weeks after germination, except for samples shown in Figure S2 where observations were performed between 6 and 8 weeks. For comparison of the fluorescence intensity between samples, the same confocal settings were used to image all meristems. Images were analyzed using Imaris 5.7 software (Bitplane AG) and Photoshop CS4 software (Adobe Systems) or MorphographX (http://www.morphographx.org).

Proper PIN:GFP expression was continuously monitored for all pML1::PIN1:GFP lines, and only plants displaying L1-specific expression were used for analysis. It is unlikely that PIN:GFP causes silencing of the endogenous PIN1 without itself being affected. Also, in the progeny of *pin1*/+, PIN1:GFP transgenic plants that no longer carry the transgene due to segregation, all of the *pin1*/+ and +/+ plants showed a wild-type phenotype. This indicates that the endogenous wild-type PIN1 copy was not stably silenced, as otherwise such progeny plants should have shown a pin-like phenotype.

Quantification of GFP Signal in the Meristems

Quantification of L1-specific GFP signal was performed using MorphoGraphX. First, surface extraction and surface cell segmentation were performed for

each meristem as described elsewhere (Kierzkowski et al., 2012). The portion of the GFP signal (1–6 μm from the extracted surface) was projected on to the resulting segmented surface. The heat maps of GFP expression in epidermal cells were then generated.

For the relative quantification of PIN1:GFP in the L1 as compared to the L2 layer, the portion of the GFP was projected on the extracted surface of the meristem and the three most recently initiated primordia (1-7 μm from the surface for the L1 and 8–15 μm for the L2) and was quantified using MorphoGraphX. For all quantifications, the area of the whole meristem and the two most recently initiated primordia were included.

Measurement of Divergence Angles

Wild-type and transgenic *Arabidopsis thaliana* plants were grown in long days for 4–6 weeks. Maximal projections of top-view confocal images of inflorescence meristem were used for all measurements. Angles between the central point of the inflorescence meristems and central points of consecutive flower meristems were measured for at least 15 plants for each line using ImageJ software (http://rsbweb.nih.gov/ij/).

Statistical Analysis

Statistical analysis was performed using Excel (Microsoft) or Matlab (Mathworks) software. Error bars in figures represent the SEM. To find the statistically significant differences, we used the Mann-Whitney U test with $p < 0.05$ as the significance level.

SUPPLEMENTAL INFORMATION

Supplemental information includes Supplemental Experimental Procedures and four figures and can be found with this article online at http://dx.doi.org/10.1016/j.devcel.2013.08.017.

ACKNOWLEDGMENTS

We are grateful to A.-L. Routier-Kierzkowska, Y. Deb, and A. Burian for comments on the manuscript; S. Gelvin, G. Morelli, and T. Vernoux for providing materials; T. Mandel for help with crosses and microscopy; and N. Signer and C. Ball for expert plant care. This work was funded by grants from the Swiss National Foundation and SystemsX.ch, the Swiss Initiative in Systems Biology.

Received: March 22, 2013
Revised: June 30, 2013
Accepted: August 22, 2013
Published: September 30, 2013

REFERENCES

Adamski, N.M., Anastasiou, E., Eriksson, S., O'Neill, C.M., and Lenhard, M. (2009). Local maternal control of seed size by KLUH/CYP78A5-dependent growth signaling. Proc. Natl. Acad. Sci. USA *106*, 20115–20120.

Baima, S., Nobili, F., Sessa, G., Lucchetti, S., Ruberti, I., and Morelli, G. (1995). The expression of the Athb-8 homeobox gene is restricted to provascular cells in Arabidopsis thaliana. Development *121*, 4171–4182.

Bainbridge, K., Guyomarc'h, S., Bayer, E., Swarup, R., Bennett, M., Mandel, T., and Kuhlemeier, C. (2008). Auxin influx carriers stabilize phyllotactic patterning. Genes Dev. *22*, 810–823.

Barbez, E., Kubeš, M., Rolčík, J., Béziat, C., Pěnčík, A., Wang, B., Rosquete, M.R., Zhu, J., Dobrev, P.I., Lee, Y., et al. (2012). A novel putative auxin carrier family regulates intracellular auxin homeostasis in plants. Nature *485*, 119–122.

Bayer, E.M., Smith, R.S., Mandel, T., Nakayama, N., Sauer, M., Prusinkiewicz, P., and Kuhlemeier, C. (2009). Integration of transport-based models for phyllotaxis and midvein formation. Genes Dev. *23*, 373–384.

Benková, E., Michniewicz, M., Sauer, M., Teichmann, T., Seifertová, D., Jürgens, G., and Friml, J. (2003). Local, efflux-dependent auxin gradients as a common module for plant organ formation. Cell *115*, 591–602.

Bilsborough, G.D., Runions, A., Barkoulas, M., Jenkins, H.W., Hasson, A., Galinha, C., Laufs, P., Hay, A., Prusinkiewicz, P., and Tsiantis, M. (2011). Model for the regulation of Arabidopsis thaliana leaf margin development. Proc. Natl. Acad. Sci. USA *108*, 3424–3429.

Blilou, I., Xu, J., Wildwater, M., Willemsen, V., Paponov, I., Friml, J., Heidstra, R., Aida, M., Palme, K., and Scheres, B. (2005). The PIN auxin efflux facilitator network controls growth and patterning in Arabidopsis roots. Nature *433*, 39–44.

Brunoud, G., Wells, D.M., Oliva, M., Larrieu, A., Mirabet, V., Burrow, A.H., Beeckman, T., Kepinski, S., Traas, J., Bennett, M.J., and Vernoux, T. (2012). A novel sensor to map auxin response and distribution at high spatio-temporal resolution. Nature *482*, 103–106.

Clough, S.J., and Bent, A.F. (1998). Floral dip: a simplified method for Agrobacterium-mediated transformation of Arabidopsis thaliana. Plant J. *16*, 735–743.

de Reuille, P.B., Bohn-Courseau, I., Ljung, K., Morin, H., Carraro, N., Godin, C., and Traas, J. (2006). Computer simulations reveal properties of the cell-cell signaling network at the shoot apex in Arabidopsis. Proc. Natl. Acad. Sci. USA *103*, 1627–1632.

Ding, Z., Wang, B., Moreno, I., Dupláková, N., Simon, S., Carraro, N., Reemmer, J., Pěnčík, A., Chen, X., Tejos, R., et al. (2012). ER-localized auxin transporter PIN8 regulates auxin homeostasis and male gametophyte development in Arabidopsis. Nat Commun *3*, 941, http://dx.doi.org/10.1038/ncomms1941.

Eriksson, S., Stransfeld, L., Adamski, N.M., Breuninger, H., and Lenhard, M. (2010). KLUH/CYP78A5-dependent growth signaling coordinates floral organ growth in Arabidopsis. Curr. Biol. *20*, 527–532.

Esau, K. (1965). Plant Anatomy. (New York: John Wiley).

Friml, J., and Jones, A.R. (2010). Endoplasmic reticulum: the rising compartment in auxin biology. Plant Physiol. *154*, 458–462.

Friml, J., Vieten, A., Sauer, M., Weijers, D., Schwarz, H., Hamann, T., Offringa, R., and Jürgens, G. (2003). Efflux-dependent auxin gradients establish the apical-basal axis of Arabidopsis. Nature *426*, 147–153.

Fujita, T., Sakaguchi, H., Hiwatashi, Y., Wagstaff, S.J., Ito, M., Deguchi, H., Sato, T., and Hasebe, M. (2008). Convergent evolution of shoots in land plants: lack of auxin polar transport in moss shoots. Evol. Dev. *10*, 176–186.

Geisler, M., Blakeslee, J.J., Bouchard, R., Lee, O.R., Vincenzetti, V., Bandyopadhyay, A., Titapiwatanakun, B., Peer, W.A., Bailly, A., Richards, E.L., et al. (2005). Cellular efflux of auxin catalyzed by the Arabidopsis MDR/PGP transporter AtPGP1. Plant J. *44*, 179–194.

Guenot, B., Bayer, E., Kierzkowski, D., Smith, R.S., Mandel, T., Žádníková, P., Benková, E., and Kuhlemeier, C. (2012). Pin1-independent leaf initiation in Arabidopsis. Plant Physiol. *159*, 1501–1510.

Heisler, M.G., and Jönsson, H. (2006). Modeling auxin transport and plant development. J. Plant Growth Regul. *25*, 302–312.

Heisler, M.G., Ohno, C., Das, P., Sieber, P., Reddy, G.V., Long, J.A., and Meyerowitz, E.M. (2005). Patterns of auxin transport and gene expression during primordium development revealed by live imaging of the Arabidopsis inflorescence meristem. Curr. Biol. *15*, 1899–1911.

Ingram, G.C. (2004). Between the sheets: inter-cell-layer communication in plant development. Philos. Trans. R. Soc. Lond. B Biol. Sci. *359*, 891–906.

Jönsson, H., Heisler, M.G., Shapiro, B.E., Meyerowitz, E.M., and Mjolsness, E. (2006). An auxin-driven polarized transport model for phyllotaxis. Proc. Natl. Acad. Sci. USA *103*, 1633–1638.

Kang, J., Tang, J., Donnelly, P., and Dengler, N. (2003). Primary vascular pattern and expression of ATHB-8 in shoots of Arabidopsis. New Phytol. *158*, 443–454.

Kierzkowski, D., Nakayama, N., Routier-Kierzkowska, A.-L., Weber, A., Bayer, E., Schorderet, M., Reinhardt, D., Kuhlemeier, C., and Smith, R.S. (2012). Elastic domains regulate growth and organogenesis in the plant shoot apical meristem. Science *335*, 1096–1099.

Kramer, E.M. (2004). PIN and AUX/LAX proteins: their role in auxin accumulation. Trends Plant Sci. *9*, 578–582.

Kuhlemeier, C. (2007). Phyllotaxis. Trends Plant Sci. *12*, 143–150.

Larson, P.R. (1975). Development and organization of the primary vascular system in Populus deltoides according to phyllotaxy. Am. J. Bot. *62*, 1084–1099.

Laskowski, M., Biller, S., Stanley, K., Kajstura, T., and Prusty, R. (2006). Expression profiling of auxin-treated Arabidopsis roots: toward a molecular analysis of lateral root emergence. Plant Cell Physiol. *47*, 788–792.

Mitchison, G.J. (1980). A model for vein formation in higher plants. Proc. R. Soc. Lond. B Biol. Sci. *207*, 79–109.

Mravec, J., Kubes, M., Bielach, A., Gaykova, V., Petrásek, J., Skůpa, P., Chand, S., Benková, E., Zazímalová, E., and Friml, J. (2008). Interaction of PIN and PGP transport mechanisms in auxin distribution-dependent development. Development *135*, 3345–3354.

Mravec, J., Skůpa, P., Bailly, A., Hoyerová, K., Krecek, P., Bielach, A., Petrásek, J., Zhang, J., Gaykova, V., Stierhof, Y.-D., et al. (2009). Subcellular homeostasis of phytohormone auxin is mediated by the ER-localized PIN5 transporter. Nature *459*, 1136–1140.

Okada, K., Ueda, J., Komaki, M.K., Bell, C.J., and Shimura, Y. (1991). Requirement of the auxin polar transport system in early stages of Arabidopsis floral bud formation. Plant Cell *3*, 677–684.

Paponov, I.A., Teale, W.D., Trebar, M., Blilou, I., and Palme, K. (2005). The PIN auxin efflux facilitators: evolutionary and functional perspectives. Trends Plant Sci. *10*, 170–177.

Parry, G., Delbarre, A., Marchant, A., Swarup, R., Napier, R., Perrot-Rechenmann, C., and Bennett, M.J. (2001). Novel auxin transport inhibitors phenocopy the auxin influx carrier mutation aux1. Plant J. *25*, 399–406.

Péret, B., Swarup, K., Ferguson, A., Seth, M., Yang, Y., Dhondt, S., James, N., Casimiro, I., Perry, P., Syed, A., et al. (2012). AUX/LAX genes encode a family of auxin influx transporters that perform distinct functions during Arabidopsis development. Plant Cell *24*, 2874–2885.

Pinon, V., Prasad, K., Grigg, S.P., Sanchez-Perez, G.F., and Scheres, B. (2013). Local auxin biosynthesis regulation by PLETHORA transcription factors controls phyllotaxis in Arabidopsis. Proc. Natl. Acad. Sci. USA *110*, 1107–1112.

Prasad, K., Grigg, S.P., Barkoulas, M., Yadav, R.K., Sanchez-Perez, G.F., Pinon, V., Blilou, I., Hofhuis, H., Dhonukshe, P., Galinha, C., et al. (2011). Arabidopsis PLETHORA transcription factors control phyllotaxis. Curr. Biol. *21*, 1123–1128.

Reinhardt, D., Mandel, T., and Kuhlemeier, C. (2000). Auxin regulates the initiation and radial position of plant lateral organs. Plant Cell *12*, 507–518.

Reinhardt, D., Pesce, E.-R., Stieger, P., Mandel, T., Baltensperger, K., Bennett, M., Traas, J., Friml, J., and Kuhlemeier, C. (2003). Regulation of phyllotaxis by polar auxin transport. Nature *426*, 255–260.

Rieu, I., and Laux, T. (2009). Signaling pathways maintaining stem cells at the plant shoot apex. Semin. Cell Dev. Biol. *20*, 1083–1088.

Rolland-Lagan, A.-G., and Prusinkiewicz, P. (2005). Reviewing models of auxin canalization in the context of leaf vein pattern formation in Arabidopsis. Plant J. *44*, 854–865.

Sablowski, R. (2011). Plant stem cell niches: from signalling to execution. Curr. Opin. Plant Biol. *14*, 4–9.

Sachs, T. (1981). The control of the patterned differentiation of vascular tissues. In Advances in Botanical Research, H.W. Woolhouse, ed. (London: Academic Press), pp. 151–262.

Sawchuk, M.G., Edgar, A., and Scarpella, E. (2013). Patterning of leaf vein networks by convergent auxin transport pathways. PLoS Genet. *9*, e1003294.

Scarpella, E., Francis, P., and Berleth, T. (2004). Stage-specific markers define early steps of procambium development in Arabidopsis leaves and correlate termination of vein formation with mesophyll differentiation. Development *131*, 3445–3455.

Scarpella, E., Marcos, D., Friml, J., and Berleth, T. (2006). Control of leaf vascular patterning by polar auxin transport. Genes Dev. *20*, 1015–1027.

Sessions, A., Weigel, D., and Yanofsky, M.F. (1999). The Arabidopsis thaliana MERISTEM LAYER 1 promoter specifies epidermal expression in meristems and young primordia. Plant J. *20*, 259–263.

Smith, R.S., and Bayer, E.M. (2009). Auxin transport-feedback models of patterning in plants. Plant Cell Environ. *32*, 1258–1271.

Smith, R.S., Guyomarc'h, S., Mandel, T., Reinhardt, D., Kuhlemeier, C., and Prusinkiewicz, P. (2006). A plausible model of phyllotaxis. Proc. Natl. Acad. Sci. USA *103*, 1301–1306.

Steeves, T.A., and Sussex, I.M. (1989). Patterns in Plant Development. (Cambridge: Cambridge University Press).

Stoma, S., Lucas, M., Chopard, J., Schaedel, M., Traas, J., and Godin, C. (2008). Flux-based transport enhancement as a plausible unifying mechanism for auxin transport in meristem development. PLoS Comput. Biol. *4*, e1000207.

Stuurman, J., Jäggi, F., and Kuhlemeier, C. (2002). Shoot meristem maintenance is controlled by a GRAS-gene mediated signal from differentiating cells. Genes Dev. *16*, 2213–2218.

Traas, J. (2013). Phyllotaxis. Development *140*, 249–253.

Tucker, M.R., Hinze, A., Tucker, E.J., Takada, S., Jürgens, G., and Laux, T. (2008). Vascular signalling mediated by ZWILLE potentiates WUSCHEL function during shoot meristem stem cell development in the Arabidopsis embryo. Development *135*, 2839–2843.

Vieten, A., Vanneste, S., Wisniewska, J., Benková, E., Benjamins, R., Beeckman, T., Luschnig, C., and Friml, J. (2005). Functional redundancy of PIN proteins is accompanied by auxin-dependent cross-regulation of PIN expression. Development *132*, 4521–4531.

Wabnik, K., Kleine-Vehn, J., Govaerts, W., and Friml, J. (2011). Prototype cell-to-cell auxin transport mechanism by intracellular auxin compartmentalization. Trends Plant Sci. *16*, 468–475.

Yadav, R.K., Girke, T., Pasala, S., Xie, M., and Reddy, G.V. (2009). Gene expression map of the Arabidopsis shoot apical meristem stem cell niche. Proc. Natl. Acad. Sci. USA *106*, 4941–4946.